



# Cascading Mechanism Triggering the Activation of Polyphenol Oxidase Zymogen in Shrimp *Litopenaeus vannamei* After Postmortem and the Correlation with Melanosis Development

Defeng Xu<sup>1</sup> · Xianqing Yang<sup>2</sup> · Yaling Wang<sup>1</sup> · Lijun Sun<sup>1</sup>

Received: 2 December 2019 / Accepted: 26 March 2020 / Published online: 3 June 2020  
© Springer Science+Business Media, LLC, part of Springer Nature 2020

## Abstract

Melanization is the major deterioration in organoleptic quality of shrimp *Litopenaeus vannamei* during cold storage and leads to dramatical reduction of commercial value. So far, the biochemical cascade mechanism triggering and accelerating melanosis progression remains unclear. Herein, this investigation aimed to monitor the melanosis development in *L. vannamei* during 5 days' cold storage at 4 °C and to explore the role of serine protease (SP) in zymogen activation of polyphenol oxidase (PPO) by application of low field nuclear magnetic resonance (LF-NMR), transmission electron microscopy (TEM), and immunohistochemistry (IHC). The results showed that melanosis development was positively associated with the increase of PPO and SP activities, and the utmost melanization was observed at cephalothorax segment, following with the telson and abdomen. Besides, LF-NMR relaxometry revealed both a dramatical reduction in trapped water component T22 and a significant increase in free water component T23. Meanwhile, the histopathological findings of hepatopancreas tissue demonstrated the progressive disruption in cytoarchitecture. Along with the increase of T23 and cytoarchitecture disruption, SP and Ca<sup>2+</sup> were arbitrarily disseminated in hepatopancreas tissue. In addition, a heat map analysis revealed that there was a highly positive relationship between melanosis development and the aberrant elevation of PPO and SP activities, ratio of T22 components, cytoarchitecture disruption level, and dissemination status of SP and Ca<sup>2+</sup>. Altogether, the biochemical cascade events for melanosis development of *L. vannamei* during cold storage could be sketched out; i.e., the cytoarchitecture disruption, in combination with the driving force of free water molecule migration, was greatly favorable for aggregation of SP, Ca<sup>2+</sup>, and PPO zymogen, following with

**Research Highlights** 1. Biochemical cascade mechanism underlying melanosis development of *L. vannamei* during storage was investigated. 2. Melanosis development was highly associated with the elevation of PPO and SP activity in hepatopancreas tissue. 3. Gradual disintegration of cytoarchitecture in hepatopancreas tissue was observed using HC and TEM. 4. Both the significant decrease in T22 and increase in T23 components were determined by LF-NMR. 5. Cytoarchitecture disruption and free water molecule migration drove dissemination of sarcoplasmic reticulum SP and Ca<sup>2+</sup>. 6. Heat map analysis demonstrated the significant correlation between melanosis development and biochemical indicators.

✉ Xianqing Yang  
yxqgd@163.com

✉ Yaling Wang  
wangylchina@163.com

<sup>2</sup> Key Laboratory of Aquatic Products Processing, Ministry of Agriculture and Rural Affairs, South China Sea Fisheries Research Institute, Chinese Academy of Fishery Sciences, Guangzhou 510300, China

<sup>1</sup> College of Food Science and Technology, Guangdong Provincial Key Laboratory of Aquatic Product Processing and Safety, Guangdong Provincial Engineering Technology Research Center of Marine Food, Key Laboratory of Advanced Processing of Aquatic Products of Guangdong Higher Education Institution, Guangdong Ocean University, Zhanjiang 524088, China

aberrant activation of PPO zymogen and initiation of melanization. These data provide new insights into the biochemical cascade mechanism of melanosis development in *L. vannamei* during cold storage and pave new ways for target controlling of melanization at initial stage.

**Keywords** *L. vannamei* · Melanization · Hepatopancreas · Cytoarchitecture disruption · SP migration

## Introduction

Pacific white shrimp (*Litopenaeus vannamei*) is one of the most widely cultivated species in the world and the melanosis or so-called dark pigmentation indicates major deterioration in quality. Melanosis usually occurs shortly after harvesting. Although melanosis is harmless to health, it dramatically devalues the commercial quality of the raw shrimps and consumers reject the products due to their unsatisfactory appearance (Chiu et al. 2007; Xu et al. 2018a, b). Therefore, melanosis is considered as a limiting factor for crustacean preservation. Theoretically, melanosis is initiated from the action of polyphenol oxidase (PPO), which consequently oxidizes phenolic compounds to quinones and spontaneously polymerizes quinones to very high molecular weight pigments (Arancibia et al. 2015; Lopez-Caballero et al. 2007; Montero et al. 2001). The melanosis development is highly related to the increase of endogenous PPO activity in shrimp and thus, the efficient inhibition of PPO activity consequently retards the melanosis development during storage (Encarnacion et al. 2012; Xu et al. 2018a, b). Even though considerable researchers have developed numerous strategies to prevent melanosis in shrimp, such as active coatings (Wang et al. 2015a, b) and high-pressure treatment (Kaur et al. 2013), refrigerated storage is still the primary method to inhibit the melanosis development (Benjakul et al. 2005; Gokoglu and Yerlikaya 2008; Encarnacion et al. 2012; Nirmal and Benjaku 2009; Somprasong et al. 2006; Wang et al. 2015a, b). Nevertheless, the preventing effectiveness of refrigerated storage on melanosis development is not yet satisfactory. Therefore, a systematical exploration into the cascade mechanism of PPO zymogen activation is an urgent prerequisite for highly efficient prevention from melanosis development under refrigerated conditions.

Melanization mediated by the prophenoloxidase (proPO)-activating system is a rapid innate immune response in invertebrates and plays a crucial role against intruding pathogens. Generally, the activation of PPO zymogen is triggered by the serine protease (SP) activation cascade system, in which the pattern recognition proteins make a complex with proPO activating enzyme(s) and microbial cell wall components and then convert proPO to active PO by limited proteolysis (Chiu et al. 2007; Luna-Acosta et al. 2011). In addition, the cation  $\text{Ca}^{2+}$  is an essential component for the binding of SP with PPO zymogen (Perazzolo and Barracco 1997; Somprasong et al. 2006). Therefore, the aggregation and

interaction of components SP,  $\text{Ca}^{2+}$ , and PPO zymogen is the prerequisite for triggering and accelerating the melanosis process. Given the significance of PPO zymogen activation in melanosis development, there is an urgent need to elucidate the biochemical events of PPO zymogen activation of shrimps during cold storage at molecular levels. For this purpose, the location and migration of the above crucial components should be clarified. Generally, SP and PPO zymogen are differentially expressed at cellular compartment, in which SP is primarily expressed at hepatopancreas tissue, whereas PPO zymogen is mostly expressed in hemolymph (Buda et al. 2005; José-Pablo et al. 2009; Luna-Acosta et al. 2011). When growing in the pond, the living shrimp *L. vannamei* response to the perturbation of external environmental stress by the innate immunity system, in which the components of PPO zymogen, SP, and  $\text{Ca}^{2+}$  are strictly regulated to interact with each other. However, after harvesting, the shrimp *L. vannamei* losses the immunity response to extracellular stress and the blood circulation is terminated. In this regard, the biochemical events of aggregation of PPO zymogen, SP, and  $\text{Ca}^{2+}$  remain unknown. In addition, although the role of SP in melanosis development of *L. vannamei* during cold storage is preliminarily explored, little information is available on the underlying mechanism of PPO zymogen activation induced by SP.

Moreover, the cytoarchitecture in living shrimp remains the integrity. Owing to the rigid compartment of organelles and other components, the migration of SP and cytosolic  $\text{Ca}^{2+}$  is rigidly restricted within the special cistes of endoplasmic reticulum, and the activation of PPO zymogen is finely regulated. Therefore, clarifying the cytoarchitecture alterations at tissue and cellular level is favorable to reveal the crucial pathway of melanosis development in *L. vannamei* during cold storage. Meanwhile, the appropriate water activity is the prerequisite for enzymatic reactions in the aqueous phase (Li et al. 2012, 2018; Sánchez-Alonso et al. 2012). However, the distribution and mobility of water molecules in stored shrimps have not been fully monitored. Thus, exploring the alteration of free water molecule distribution is favorable to understand the driving force of SP and  $\text{Ca}^{2+}$  migration in *L. vannamei* during cold storage. Furthermore, the overall correlation analysis between melanosis development and biochemical indicators is certainly a potent tool to demonstrate interactions between the elevation of PPO and SP activities, alteration of cytoskeleton morphology, distribution of water molecules, and migration of SP and  $\text{Ca}^{2+}$ .

Therefore, to elucidate the biochemical mechanism of PPO zymogen activation and to determine the crucial step for melanosis target control, the melanosis development and its correlation with PPO and SP activities were explored. Then, the alterations of cytoskeleton, distribution of water molecules, and migration of SP and  $\text{Ca}^{2+}$  during melanosis development were systematically investigated with low field nuclear magnetic resonance (LF-NMR), transmission electron microscopy (TEM), and immunohistochemistry (IHC). Furthermore, the heat map analysis based on Pearson correlation was used to visualize the underlying biochemical mechanism for the activation of PPO zymogen. This research provides a deeper insight into melanosis development in *L. vannamei* during cold storage and has the potential to conceptualize innovative ways to control melanization.

## Materials and Methods

### Shrimp Collection and Storage

600 live *L. vannamei* with the average weight of  $20.45 \pm 2.16$  g and length of  $12.69 \pm 1.78$  cm were purchased from a local shrimp culture pond of Zhanjiang city, China. The live shrimps were transported to the laboratory at the College of Food Science and Technology, Guangdong Ocean University, within 1 h. Upon arrival, shrimps were washed in the clean tap water and the shrimps with signs of visual defects or damage were discarded. The selected shrimps were packed in sterile Reynolds zipper ( $26.8 \times 27.9$  cm) polyethylene bags (Alcoa Products Inc., Richmond, VA 23261, USA) and stored at temperature of 4 °C. Generally, the quality deterioration progression of shrimp during refrigerated storage was monitored every day (Alparslan and Baygar 2017; Dai et al. 2016; Kaur et al. 2013; Nirmal and Benjaku 2009; Wang et al. 2015a, b). Therefore, according to the previous reports, 6 of shrimps were randomly sampled out for intervals of 24 h and the quality deterioration indicators, such as sensory score, brightness, activities of PPO and SP, disruption of cytoarchitecture, distribution of water molecule components, and pathological dissemination of SP and  $\text{Ca}^{2+}$  in hepatopancreas tissue, were determined, respectively. To illuminate the experimental design of present study, an overview framework is shown in Fig. 1.

### Determination of Sensory Quality

The overall sensory score was assessed according to the method described by Alparslan and Baygar (2017) and Xu et al. (2018a, b) with slight modifications. The sensory panel consisted of 10 trained assessors from our laboratory staff. For every 24-h interval, 6 of the shrimps were fetched out

from the refrigerated compartments and subjected to overall sensory assessment. The panelists were asked to assign a score of 1–10 (1 = dislike extremely, 2 = dislike very much, 3 = dislike moderately, 4 = dislike slightly, 5 = neither like nor dislike, 6 = like slightly, 7 = like moderately, 8 = like very much, 9 = like extremely, 10 = excellent) for each shrimp on appearance, color, odor, and texture. The evaluation by a panel of assessors was analyzed statistically and the storage time of sensory rejection was defined as the time when the overall sensory score is below 5.

### Determination of Melanosis Development

The cephalothorax segment of a whole shrimp was selected for color measurement. The melanosis development was periodically evaluated by determination of values brightness ( $L^*$ ), redness ( $+a^*$ ), and yellowness ( $+b^*$ ) with a Hunter Lab Ultra Scan PRO colorimeter (Hunter Associates Laboratory, Inc., Reston, VA, USA). The Hunter Lab color meter was calibrated using black and white references. The detection of CIELAB parameters  $L^*$  was carried out according to the method by Dai et al. (2016) and Encarnacion et al. (2012).

### Preparation of PPO and SP Crude Extract

Cephalothorax including the first three thoracic segments was separated from the whole shrimps and this tissue was immediately mixed with dry ice. Then, the cephalothorax tissue was pulverized by grinding in a coffee mill and the powder was stored at  $-80$  °C for crude enzyme extraction. To extract PPO, 50 g of powder was mixed with 150 mL of 50 mM sodium phosphate buffer (pH 7.2), containing 1.0 M NaCl, 0.2% Brij 35, and 2% polyvinylpyrrolidone (PVPP) according to the method of Manheem et al. (2012) with slight modifications. To prevent the activation of PPO zymogens during PPO extraction, the irreversible SP inhibitor of 2 mM phenylmethylsulfonyl fluoride (PMSF) was added into the extraction buffer. The mixture was stirred continuously at 4 °C for 30 min, followed by refrigerated centrifugation at  $8000 \times g$  for 30 min using a centrifuge (Beckman Coulter, Avanti J-E Centrifuge, Fullerton, CA, USA). Solid ammonium sulfate was added into the supernatant to obtain 40% saturation. The mixture was allowed to stand at 4 °C overnight and then centrifuged at a speed of  $12,000 \times g$  and 4 °C for 30 min. The obtained pellet was collected and dispersed in a minimum volume of 50 mM sodium phosphate buffer (pH 7.2). The pellet solution was dialyzed against 15 volumes of the same buffer at 4 °C overnight. After dialysis, insoluble materials in the dialysate were removed by centrifugation at  $3000 \times g$  and 4 °C for 30 min and the supernatant was named the crude PPO extract. SP extraction was conducted according to the procedures of PPO extraction but the irreversible

inhibitor PMSF for SP was removed from the sodium phosphate buffer.

### Measurement of PPO and SP Activities

PPO activity was determined spectrophotometrically using a TU-1810 spectrophotometer (Beijing Purkinje General Instrument Ltd., China) according to the method of Xu et al. (2018a, b) and Romano et al. (2015) with some modifications. Briefly, the reaction mixture containing 50  $\mu\text{L}$  of crude PPO extract and 700  $\mu\text{L}$  of 10 mM DL-3,4-dihydroxyphenylalanine (DL-DOPA) in 50 mM sodium phosphate buffer (pH 6.5) was incubated at 35 °C and the absorbance at 475 nm was measured every 15 s during 10 min. One unit of enzymatic activity was defined as an increase in absorbance of 0.001 per minute. Experiments were performed in triplicate, and the results were expressed as units of enzymatic activity per mg of protein. The protein content was measured according to the method of Bradford (1976) using bovine serum albumin as standard.

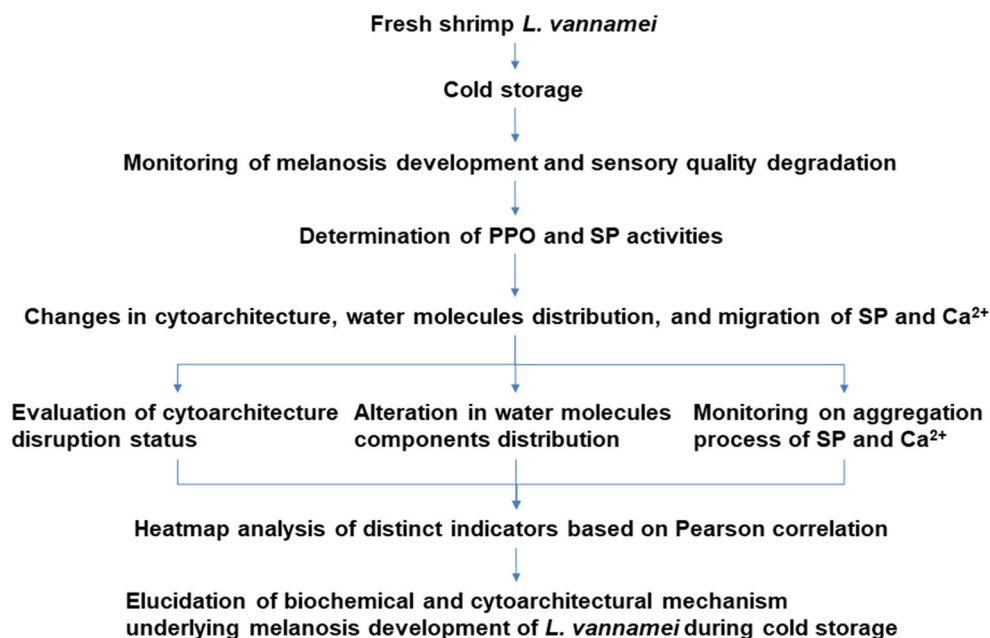
SP activity assay was determined according to the method described by Liu et al. (2017) with some modifications. The reaction mixture contained 600  $\mu\text{L}$  of 15 mM fluorescent substrate in deionized water, 400  $\mu\text{L}$  of 50 mM Tris-HCl buffer (pH 8.0), 100  $\mu\text{L}$  of deionized water, and 5 mM dithiothreitol. These reagents were preincubated at 37 °C for 30 min and then the enzymatic reaction was initiated by adding 100  $\mu\text{L}$  of crude SP extract and kept for 30 min. The hydrolysis efficiency of SP was determined against suc-ala-ala-pro-phe-pNA (CAS No. 70967-97-4, Sigma, USA). The formation of pNA was monitored by measuring the absorbance at 405 (A405) nm using a TU-1810 spectrophotometer (Beijing

Purkinje General Instrument Ltd., China). One unit of SP activity is defined as an increase in A405 by 0.01/min/mL. Enzyme and substrate blanks were prepared by excluding the substrate and enzyme, respectively, from the reaction mixture and deionized water was used as control.

### Histochemistry and Electronic Microscopy Observation of Hepatopancreas Tissue

For histochemistry analysis, 6 shrimps were randomly taken from the polyethylene bags every day and the hepatopancreas tissue was delaminated out of the whole shrimp as described by Li et al. (2008) and Romano et al. (2015) with some modifications. In this procedure, the hepatopancreas tissue was immersed into Bouin's solution for 48 h and then transferred to an ethanol solution with concentration gradients of 70, 90, and 100% (v/v) to displace the water. Afterwards, the dehydrated tissue was infiltrated with wax and embedded into wax blocks. The sections with 7  $\mu\text{m}$  of thickness were made using a rotary microtome (Leica, RM2235, Germany) and stained with hematoxylin and eosin. The morphology of hepatopancreas tissue was observed and photographed under a light microscope ( $\times 200$  magnification). The overall morphology and microstructure degradation of hepatopancreas tissue and organelles were further characterized by transmission electron microscopy (TEM). The ultrastructure sections of hepatopancreas tissue were prepared according to the method described by Xu et al. (2018a, b) with some modifications. Briefly, the hepatopancreas was cut into small portions (0.2 cm  $\times$  0.2 cm  $\times$  0.2 cm), fixed in 2.5% glutaraldehyde for 24 h, and transferred to a phosphate buffer (pH 7.4, 0.1 M, 4 °C). Then, it was fixed in 2% osmium tetroxide in 0.1 M

**Fig. 1** The schematic overview of the experimental design



phosphate buffer (4 °C) for 1.5 h before dehydration in gradient concentrations of ethanol solutions (50, 70, 90, 95, and 100%). The dehydrated samples were embedded in epoxy resin (Epoxy Embedding Medium Kit, Sigma) and then cut to ultrastructure sections of 70 nm using the Leica Ultracut UCT25 ultramicrotome. Ultrathin sections were stained by lead citrate and uranyl acetate and then observed using a Hitachi H500 TEM.

### Monitoring of Water Molecular Distribution

The distribution of water molecule was monitored by LF-NMR as described by Sánchez-Alonso et al. (2014), Han et al. (2014), and Shao et al. (2016) with some modifications. The surface water in the shrimp sample was gently wiped off to reduce the interfering signal. Then, the shrimp was placed inside the cylindrical glass tubes (60 mm in diameter) for about 10 min until it was equilibrated to 32 °C. The measurements of the transverse relaxation time (T<sub>2</sub>) were performed on a Meso MR-60 Pulsed NMR analyzer (Niuman Electric Corporation, Shanghai, China) with a magnetic field strength of  $0.5 \pm 0.05$  T corresponding to a proton resonance frequency of 23.3 MHz. The T<sub>2</sub> was measured using Carr-Purcell-Meiboom-Gill (CPMG) with 32 scans, 12,000 echoes, 6.5 s between scans, and 200 μs between pulses of 90 and 180°. The LF-NMR relaxation curve was fitted to a multi-exponential curve with the MultiExp Inv Analysis software (Niuman Electric Corporation, Shanghai, China), using the inverse Laplace transform algorithm. The parameters of T<sub>2</sub> were the relaxation components. Additionally, the width of the relaxation amplitude was calculated between the relaxation time of the start and the end of peaks. After LF-NMR measurement, <sup>1</sup>H MRI images of shrimp were acquired on an MR23-060 H<sup>1</sup>-NMR Analyzer by using the multiple-spin-echo (MSE) sequence as described by Li et al. (2018). After unified mapping and pseudocolor processing, the gray images were subsequently changed into color ones. Finally, the proton density of the weighted images of water molecular mobility and distribution was clearly presented as color images.

### Localization of SP and Ca<sup>2+</sup> in *L. vannamei* Hepatopancreas

Distribution of SP and Ca<sup>2+</sup> in *L. vannamei* hepatopancreas tissue was monitored by IHC according to the procedures described by Wu et al. 2008 and Nunes et al. (2014). The dehydrated paraffin specimen sections of hepatopancreas tissue were incubated in distilled water with protein kinase K 20 μg/μL for 20 min at 37 °C. Endogenous peroxidase activity of tissues was blocked in TBS-T with 3% hydrogen peroxide (Sigma-Aldrich) for 30 min. To prevent nonspecific reactions, tissue sections were incubated with 10% normal bovine serum albumin at room temperature overnight. After

blocking in a buffer (1% BSA and 5% normal goat serum in TBS-T) for 2 h, the sections were incubated with the primary SP antibodies (PRS45, Sigma-Aldrich) at 4 °C overnight. On the second day, the slides were rinsed with TBS-T twice for 5 min and then incubated with HRP-conjugated goat anti-rabbit antibodies (Alpha Diagnostic, San Antonio, TX, USA) for 1 h. Slides were stained with 3,3'-diaminobenzidine (DAB, R&D Systems, Minneapolis, MN, USA). After DAB staining, the slides were rinsed with distilled water and dehydrated with 70, 95, and 100% ethanol solution twice for 3 min, respectively. The dehydrated slides were hyalinization in xylene twice and finally mounted with Cytoseal™ (Thermo Scientific, Waltham, MA, USA). Localization of Ca<sup>2+</sup> was performed according to the method described by Ahn et al. (2017) with some modifications. Sections were incubated with Flur-2 Ca<sup>2+</sup> fluorescent probe for 30 min. The presentative images were observed and photographed using a fluorescent microscope (IX70, Olympus).

### Statistical Analyses

The experiments were randomly designed and all data were expressed as mean ± standard deviation (SD). Statistical analysis was performed using a SPSS package (SPSS 11.0 for windows, SPSS Inc., Chicago, IL, USA). The Pearson correlation coefficient was calculated to find correlations between the indicators with a significant difference. Analysis of variance (ANOVA) was performed and the mean comparisons were made by Duncan's multiple range test. For pair comparison, *T* test was used. Heat map analyses of the resulting data matrix were performed with R language (version 3.3.1) which is available from <https://cran.r-project.org/web/packages/pheatmap/>.

## Results and Discussion

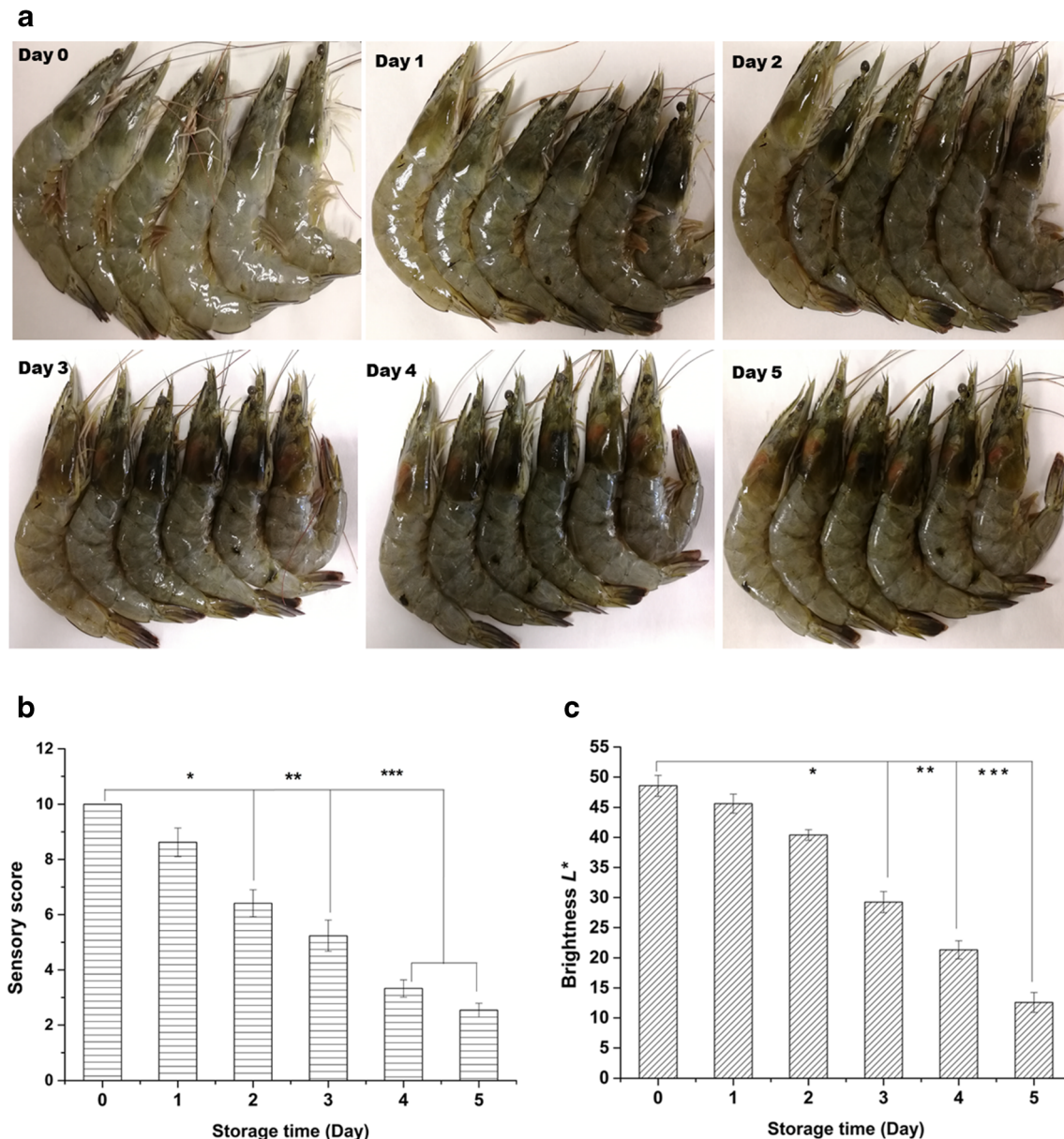
### The Melanosis Development of *L. vannamei* During Cold Storage Was Observed at Susceptible Segments and Time Nodes

Figure 2 illustrated the changes in overall sensory quality and melanosis development of *L. vannamei* during 5 days of cold storage. As shown in Fig. 2a, b, all the shrimps were desirable in sensory quality and the overall sensory score was 10 at the initial stage. With the prolongation of storage, however, the overall sensory quality began to degradation and the sensory score slightly reduced from 10 on day 0 to  $6.41 \pm 0.49$  on day 2. Notably, the remarkable deterioration in sensory quality was observed on day 3 and the overall sensory score dropped to  $5.24 \pm 0.56$ . Afterwards, the sensory score sharply decreased to  $3.33 \pm 0.31$  on day 4 and  $2.54 \pm 0.25$  on day 5, respectively. Meanwhile, the unpleasant odor and texture softening were

observed. In regard to the melanosis development, the appearance of shrimps was almost transparent and the values of brightness  $L^*$  were above 40 during the first 2 days of cold storage. However, the values underwent a linear decline on day 3 and continuously dropped to  $12.58 \pm 1.65$  at the end of storage (Fig. 2c). Furthermore, the utmost melanization was observed at cephalothorax segment, followed by the stern and abdomen. This phenomenon indicated that most violent biochemical reaction took place in cephalothorax segment and the underlying biochemical mechanism deserved to explore at cephalothorax.

Considerable pieces of evidence have demonstrated that melanization is induced by a complex enzymatic

cascade and involves the activation of PPO zymogens through limited proteolysis by endogenous serine proteases (Alparslan and Baygar 2017; Chiu et al. 2007; Montero et al. 2001; Nirmal and Benjaku 2009; Perazzolo and Barracco 1997). Obviously, the activation of PPO zymogens is largely responsible for the development of melanosis. However, after harvesting, the cascading events between PPO zymogen and SP have not yet been investigated. Therefore, exploring the role of SP in the cascade events of PPO zymogen activation would certainly be favorable in targeting control of shrimp melanosis development during cold storage.



**Fig. 2** Sensory degradation proceedings of *L. vannamei* during cold storage for 5 days' storage. **a** Appearance deterioration; **b** overall sensory deterioration; **c** melanosis development. The marks of \*, \*\*,

and \*\*\* denote significant differences as compared with the initial day at  $P < 0.05$ ,  $P < 0.01$ , and  $P < 0.001$  levels, respectively

### Elevation of PPO Activities Was Highly Associated with the Increase of SP Activity in *L. vannamei* During Cold Storage

As shown in Fig. 3a, the PPO activities in cephalothorax elevated with the prolongation of storage time and the great majority of PPO activity (more than 90%) was determined on day 3. On the initial stage of storage, few PPO zymogen was activated and the PPO activity was  $173.18 \pm 15.71$  U/mg protein on day 1 and a moderate rise when compared with the value of  $124.27 \pm 16.33$  U/mg protein on day 0. Thereafter, PPO activity elevated rapidly and reached to  $265.21 \pm 21.14$  U/mg protein on day 2,  $292.38 \pm 23.11$  U/mg protein on day 3,  $314.53 \pm 15.66$  U/mg protein on day 4, and  $328.69 \pm 29.75$  U/mg protein on day 5, respectively. This significant elevation of PPO activity indicated that the PPO zymogen was progressively activated with the prolongation of storage.

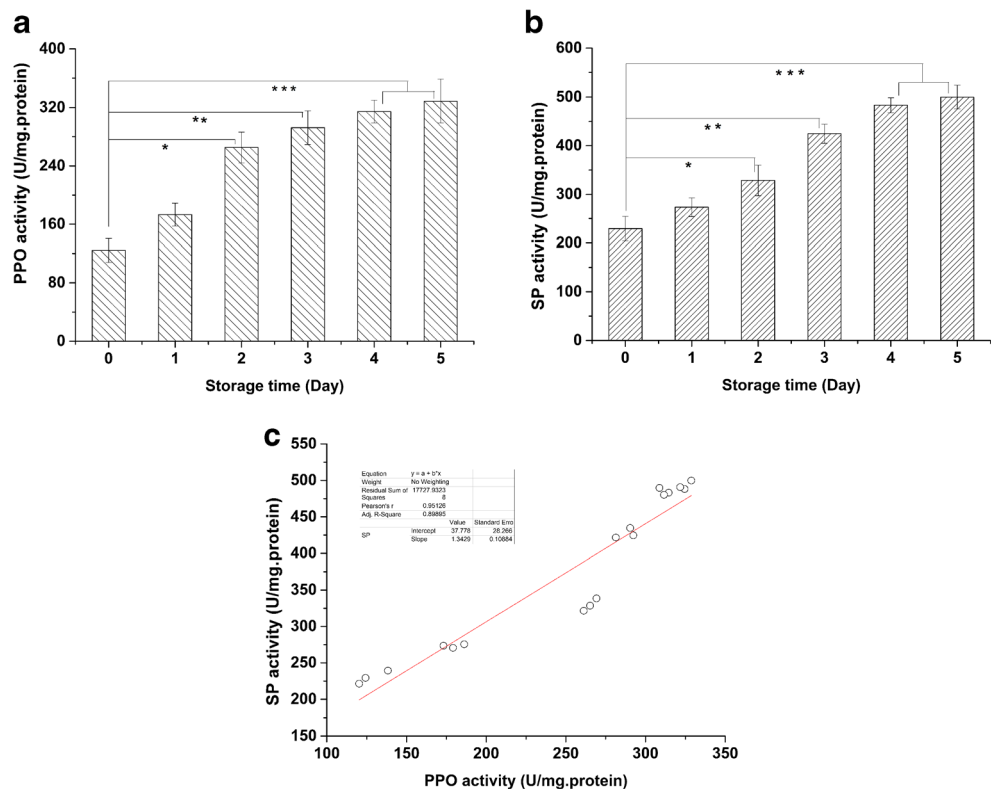
Furthermore, in view of the cascade biochemical reaction between PPO zymogen and SP in shrimp’s innate immunity system (Amparyup et al. 2007; Jiang et al. 2003; Visetnan et al. 2009), it is necessary to elucidate the changing profiles of SP activities and to analyze its correlation with PPO activities during cold storage. As illustrated in Fig. 3b, SP activity gradually elevated with the increase of storage and presented a similar tendency to PPO activities. On day 0, SP activity was determined at  $229.38 \pm 25.12$  U/mg protein and raised to

$273.56 \pm 19.35$  U/mg protein on day 1. Afterwards, the SP activity further ascended and reached a significantly higher level when compared with that of day 0 ( $P < 0.05$  or  $P < 0.01$  or  $P < 0.001$ ). Besides, the correlation analysis illustrated the positive coefficient of 0.95 between PPO and SP activities (Fig. 3c), suggesting the involvement of SP in the process of PPO activation in *L. vannamei* hepatopancreas tissue during cold storage.

### The Hepatopancreas Tissue of *L. vannamei* Was Subjected to a Gradual Disruption During Cold Storage

In living shrimps, the morphology of hepatopancreas tissue was plump and the texture was elastic. During postmortem storage, however, the morphology of hepatopancreas tissue was progressively deteriorated. As shown in Fig. 4a, the hepatopancreas tissue remained the plump shape and elastic texture on the initial stage of storage. Nevertheless, gradual intensifying was observed and the distinct postmortem proteolysis appeared on day 3. Afterwards, the postmortem autolysis accelerated and the significant tissue autolysis was observed on day 5. Based on the occurrence of rapid autolysis in hepatopancreas tissue, it could infer that the intercellular connections were subjected to disruption during cold storage. Besides, to gain deep insight into the biochemical mechanism

**Fig. 3** Activity elevation and correlation of melanosis-related endogenous enzymes in *L. vannamei* hepatopancreas tissue during cold storage for 5 days’ storage. **a** Elevation of PPO activity; **b** elevation of SP activity; **c** correlation between PPO and SP activity. The marks of \*, \*\*, and \*\*\* denote significant differences as compared with the initial day at  $P < 0.05$ ,  $P < 0.01$ , and  $P < 0.001$  levels, respectively



of melanosis development from the perspective of cytoarchitecture fragmentation, it is favorable to elucidate the histological deterioration in *L. vannamei* hepatopancreas segments during cold storage.

The morphological change of transverse paraffin sections in hepatopancreas tubules was illustrated in Fig. 4b. On day 0, the hepatopancreas tissue was composed of many hepatopancreas tubules which are regularly assembled and well organized to each other in the lumina. The integrity of intercellular connections was well conserved, surrounding the hepatopancreas tubule. With the increase of storage time, however, the significant disruption of intercellular connections in tubule lumina was observed. On day 1, hepatopancreatic tubules were slightly sloughed off from the epithelial lining and the cell content was dispersed in the tubule lumen. On day 2, the stellate tubule lumen was dramatically autolyzed and some intercellular connections disappeared. Afterwards, the intercellular connections were completely decomposed and the hepatopancreas cells were consequently sloughed off from epithelial lining. With the further prolongation of storage, the fragile hepatopancreas cells significantly underwent autolysis and the complete disintegration was observed on day 5. In a word, this cytoskeleton deterioration of intercellular connections in hepatopancreas tissue indicated that the integrity of barrier structure suffered from fragmentation during cold storage.

Furthermore, the above fragmentation in intercellular connections of hepatopancreas tissue was quantitatively evaluated

with the Image J software (1.52n, National Institutes of Health) and the result was shown in Fig. 4c. On day 0, the shrinkage area caused by intercellular connection fragmentation in hepatopancreas tissue was only  $(18.54 \pm 2.11) \times 10^{-2} \text{ mm}^2$ . With the prolongation of storage, however, the area sharply increased and the significant levels were observed. Exactly, compared with the value on day 0, the values increased to  $(31.37 \pm 2.33) \times 10^{-2} \text{ mm}^2$  on day 2 and  $(43.23 \pm 2.18) \times 10^{-2} \text{ mm}^2$  ( $P < 0.05$ ) on day 3, respectively. On day 4, the ruptured area further elevated to  $(53.77 \pm 1.97) \times 10^{-2} \text{ mm}^2$  with  $P < 0.01$ , and the highest value of  $(73.63 \pm 3.89) \times 10^{-2} \text{ mm}^2$  was found on day 5 ( $P < 0.001$ ). Together, these findings quantitatively demonstrated the disruption progression of hepatopancreas tissue of *L. vannamei* during cold storage.

Moreover, TEM findings provide further information for understanding the biochemical mechanism of melanosis development from the perspective of membrane structure degradation. As shown in Fig. 5, on day 0, large numbers of organelle components, such as ribosomes (R), endoplasmic reticulum (ER), nucleus (N), mitochondria (M), and vesicles (V) in hepatopancreas tissue exhibited clear ultrastructure and the membrane structure remained the integrity, which were illustrated by the dotted line. However, the membrane structure of organelle components gradually disrupted with storage prolonging. On day 1, the slight disruption of ultrastructure was observed. Exactly, the membrane of ER and M suffered from gradual damage and the organelle inclusions were

**Fig. 4** Typical shrinkage changes in *L. vannamei* hepatopancreas tissue during cold storage for 5 days' storage. **a** Macro-morphological changes; **b** changes in overall tubules structure, the black arrows point to the necrocytosis and the dissemination of organelle components; **c** changes in shrinkage area. The marks of \*, \*\*, and \*\*\* denote significant differences as compared with the initial day at  $P < 0.05$ ,  $P < 0.01$ , and  $P < 0.001$  levels, respectively

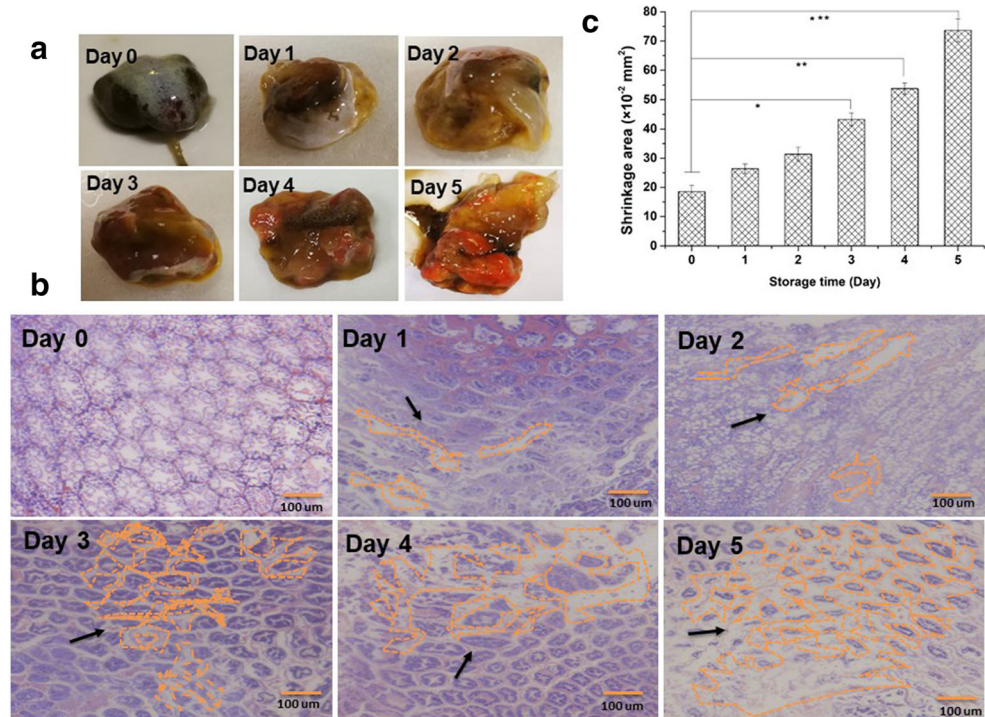
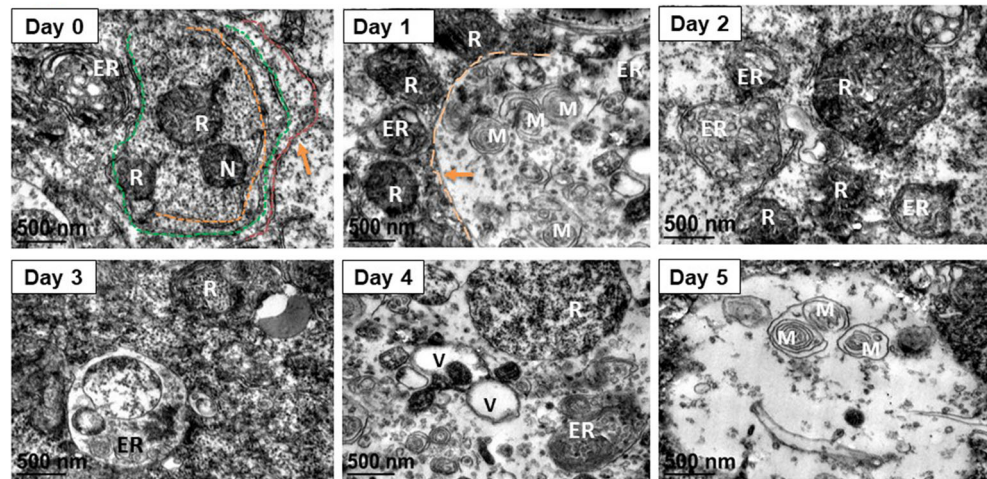




**Fig. 5** Typical TEM images of *L. vannamei* hepatopancreas tissue during cold storage for 5 days' storage. The orange arrows point to the disruption of cytoarchitecture membrane system and the dissemination of organelle components



consequently scattered in the cell lumen. In addition, the compartment membrane between organelle components underwent obvious fragmentation and disruption. Afterwards, the compartment membrane was completely disrupted and the disruption in organelle ultrastructure was greatly accelerated. On day 3, the significant disruption of ultrastructure membrane was observed and the mitochondria ultrastructure was completely decomposed. On day 4, the fusion of organelle was further progressed and the significant loss of compartments was observed on day 5.

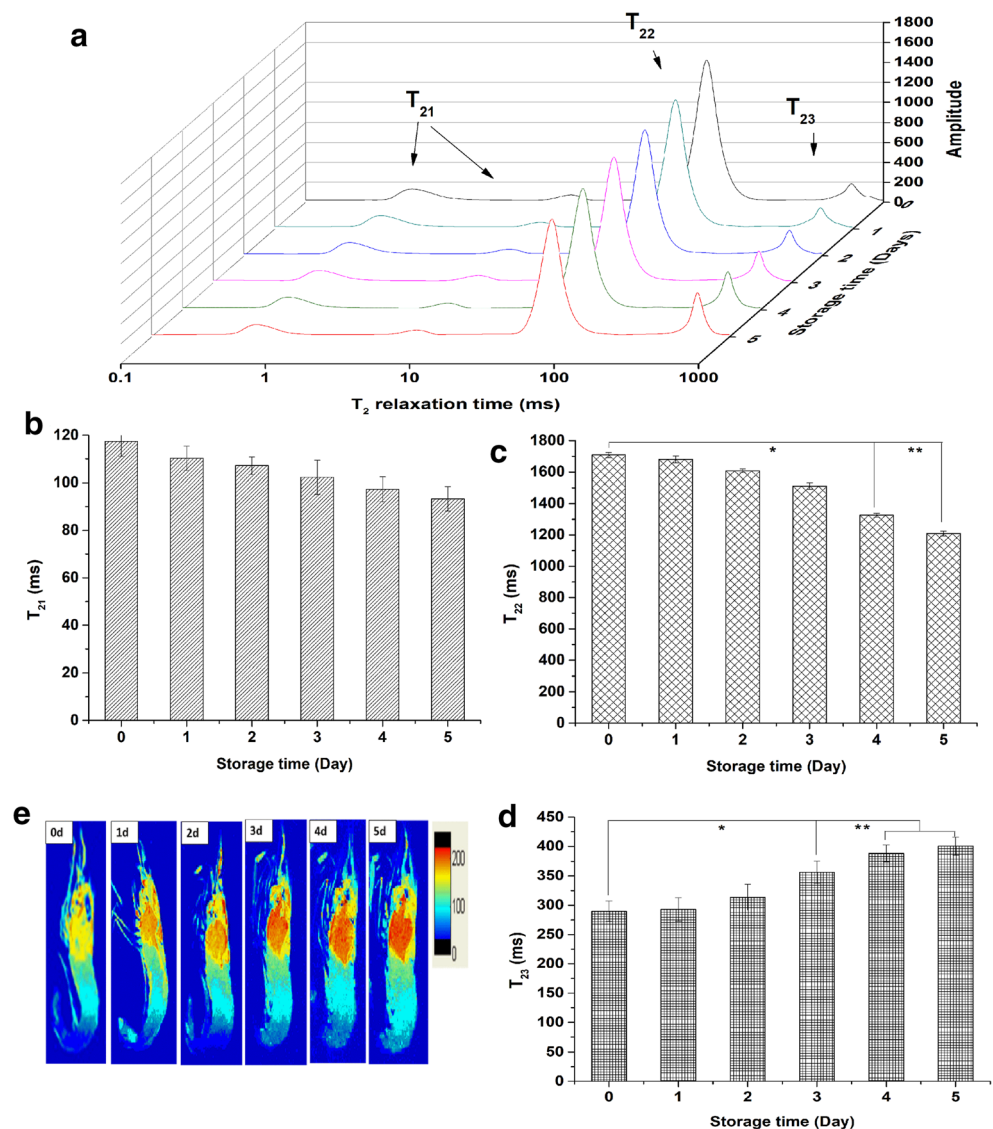
Generally, the cellular compartments separate the contact between the cytoarchitecture and hydrolase and thus confer the normal morphology of tissue framework. As for shrimp species, SP is primarily expressed at hepatopancreas tissue, whereas PPO zymogen is exclusively expressed in hemolymph (Buda et al. 2005; José-Pablo et al. 2009; Luna-Acosta et al. 2011). At living state, the contact of PPO zymogen with SP is primarily inhibited by cellular compartment and the interaction between PPO and SP is accurately regulated in response to the environmental stress. After postmortem, however, the abundant hydrolase is extremely inclined to releasing from lysosomes and breakdown macromolecules into smaller subunits. As a result, the cytoskeleton is disrupted and the texture is lost. In this study, the plump shape and elastic texture of hepatopancreas tissue in *L. vannamei* gradually were subjected to decomposition with the increase of storage (Fig. 4a). In addition, the significant disruption of intercellular connections between tubules demonstrated the involvement of hydrolase in disintegration of hepatopancreas tissue (Fig. 4b). Furthermore, the disruption of membrane ultrastructure of organelle components indicated the loss of intercellular compartments (Fig. 5). As a whole, these disruption and fragmentation events occurring on cellular structure would consequently lead to the degeneration of hepatopancreatic tubule apices and facilitate the immediate contact of SP with PPO zymogens.

### Disruption of Cytoskeleton Facilitated the Mobility of Free Water Molecules in Hepatopancreas Tissue of *L. vannamei* During Cold Storage

Appropriate content of free water molecules is necessary for the enzymatic reaction in aqueous phase. As described by Li et al. (2018), the distribution of water molecules both in free and bound state in prawns could be investigated by measuring the spin-spin relaxation time T<sub>2</sub> of water protons using LF-NMR. As shown in Fig. 6a, the T<sub>2</sub> spectrum in the shrimp sample was constituted of four distinct components. A minor and fastest relaxing component T<sub>21</sub> with relaxation times in the range from 0.1 to 10 ms contained two peaks, which accounted for about 5% of the total signal. Liu et al. (2015a, b) attributed this component T<sub>21</sub> to hydrate water owing to the combining of the proteins and unavailability to the biochemical reaction. The third peak T<sub>22</sub> accounted for about 90% of the total signal and covered a relaxation time in the range of 10–100 ms with centering at 40–70 ms. As for this dominant component, Li et al. (2014) indicated that this component was possibly trapped in the myofibrils and assigned it intermediate water. The fourth peak T<sub>23</sub> in water molecule relaxing time plot was the slowest component with a relaxation time in the range of 200–1000 ms and accounted for about 5% of the total signal. Liu et al. (2016) considered this component T<sub>23</sub> to be the free water molecules because of the localization out of the cellular framework and necessity for the enzymatic reaction.

The relative abundance and distribution of bound water component T<sub>22</sub> and free water component T<sub>23</sub> in the food matrix reflected the mobility of water molecules and had a direct influence on the speed of the enzymatic reaction and quality degradation. Figure 6a further illustrated the overall changes in the water molecule distribution of *L. vannamei* during cold storage. Within the entire storage period of 5 days, no significant difference was found in component T<sub>21</sub>, although there was a gradual decrease tendency from day 0 to day 5 (Fig. 6b). However, the significant changes were

**Fig. 6** Alteration of water molecule distribution on T2 relaxation times in *L. vannamei* during cold storage for 5 days' storage. **a** Overall distribution of water molecule components; **b** distribution of hydrate water molecule components T21; **c** distribution of bonding water molecule components T22; **d** distribution of free water molecule components T23; **e** visualization of proton density-weighted images of water molecules. The marks of \*, \*\*, and \*\*\* denote significant differences as compared with the initial day at  $P < 0.05$ ,  $P < 0.01$ , and  $P < 0.001$  levels, respectively



observed in T22 and T23. As shown in Fig. 6c, on the initial stage of storage, the amplitude of T22 was determined to be  $1708.45 \pm 16.37$  ms and gradually declined since then. On day 4 and day 5, the values dropped by  $1325.83 \pm 13.24$  ms and  $1208.75 \pm 15.21$  ms, respectively, significantly lower than that of day 0 ( $P < 0.05$  or  $P < 0.01$ ). On the contrary, the relative abundance of T23 component significantly increased (Fig. 6d). In comparison with the amplitude T23 of  $289.69 \pm 17.45$  ms in fresh shrimp, the value of  $356.28 \pm 19.28$  ms on day 3 was significantly higher ( $P < 0.05$ ). In addition, a further increase of T23 component was found, with the values of  $388.15 \pm 14.23$  ms on day 4 and  $400.49 \pm 15.11$  ms on day 5, both maintaining the level of  $P < 0.01$ . Altogether, these remarkable changes in T22 and T23 clearly demonstrated that the mobility of free water molecules in *L. vannamei* significantly increased during the cold storage, which accordingly provided a driving force for migration of PPO zymogens and aggregation with SP.

Furthermore, the proton density-weighted images of T2 components were acquired using the multiple-spin-echo sequence. This image not only determines the free water distribution in samples but also indirectly visualizes the structure changes during processing (Geng et al. 2015). In this work, proton density image was chosen to reflect the distribution changes in free water molecules. Owing to the lower proportion of bound water, the intermediate and free water molecules (T22 and T23) were visible in the images and represented the most abundant water in shrimp samples. To clearly visualize the mobility of water molecules, a color bar was used to scale the density of water protons, in which the red color referred to the higher density of protons and indicated higher mobility of water molecules while the blue one referred to the lower density of free water protons. As shown in Fig. 6e, significant difference in distribution of free water protons was observed between the cephalothorax, abdomen, and stern segments. In comparison with the abdomen and stern segments, the proton

density image in the cephalothorax location was observed with orange and red color, indicating a major accumulation site of free water molecules. Additionally, compared with the images of fresh shrimps, the sample images with different times of storage presented a gradual increase in intensity of red color, indicating the increase of water mobility towards cephalothorax location.

Actually, it is well known that there remains a high association between the food matrix microstructure and water mobility. The disruption of cellular integrity would certainly lead to an increase in water mobility (Sánchez-Alonso et al. 2012). Therefore, this distribution changes in bound water and free water molecules reflect the cytoarchitecture deterioration in hepatopancreatic tissue. LF-NMR is a rapid and non-destructive detection method which requires only minimal or no sample preparation to produce characteristic fingerprints for a given sample. Based on the rapid and non-destructive measurement of transverse water proton relaxation, LF-NMR spectroscopy has been widely used to evaluate the property changes during food storing or processing stage (Erikson et al. 2004; Liu et al. 2015a, b; Sánchez-Alonso et al. 2014; Sánchez-Valencia et al. 2014). In this study, the overall T2 relaxometry profiles revealed the characteristic distribution of free water molecules in *L. vannamei* during cold storage and indirectly indicated the location of PPO activity.

### The Disruption of Cytoskeleton and Migration of Free Water Molecules Drove the Migration of SP and Ca<sup>2+</sup> in Hepatopancreas Tissue of *L. vannamei* During Cold Storage

In living shrimp, the activation of PPO zymogen is mediated by SP clip domain and the level of PPO activities is under the control of SP activation cascade (Liu et al. 2015a, b). Furthermore, with the identification of various serpins in shrimps, the PPO activation can be blocked by inhibiting SP activities in plasma, which clearly demonstrates the involvement of SP in activation of PPO zymogen (Perazzolo and Barracco 1997; Liu et al. 2016; Jiang et al. 2003). SP was mainly expressed at the hepatopancreas tissue, whereas the PPO was primarily produced in the carapace and hemocytes of shrimp (José-Pablo et al. 2009; Luna-Acosta et al. 2011). Buda et al. (2005) found that the SP gene was mostly transcribed in the hepatopancreas tissue and a low level was detected in the hemocytes. Therefore, understanding the migration of SP activity in *L. vannamei* during cold storage would be pivotal for elucidating the biochemical mechanism of melanosis development. Figure 7a illustrated the migration of SP activity in hepatopancreas tissue of *L. vannamei* during cold storage. On the initial stage of storage day 0, the morphology of cellular architecture was integrity and the majority of SP was localized at the intracellular boundary. During the first 2 days of storage, the gradual migration of SP activity

from intracellular to extracellular space was observed and the most remarkable diffusion was found on day 4. Afterwards, in combination with the disruption of intracellular boundary, the majority of SP activity was completely released and disseminated throughout the hepatopancreas tissue.

Moreover, Perazzolo and Barracco (1997) and Reis et al. (1999) found that SP activity was cation-dependent and 5 mM of Ca<sup>2+</sup> were the optimal concentrations for performing SP biochemical functions. Generally, Ca<sup>2+</sup> is mainly distributed in the cytoplasm and cannot be freely translocated to the intercellular membrane (Liu et al. 2016). Fura-2 is a commonly used fluorescent dye for Ca<sup>2+</sup> determination and is used as a histochemical marker for the localization of Ca<sup>2+</sup>. As shown in Fig. 7b, in fresh shrimp samples, the cellular architecture was intact and the cation of Ca<sup>2+</sup> was mostly localized in cytoplasm. With the increase of storing time, the Ca<sup>2+</sup> began to migrate from cytoplasm to extracellular space due to the rupture of cytoplasm membrane, and the most remarkable migration was found on day 4 of storage. In view of the disruption of cellular integrity in hepatopancreas tissue of *L. vannamei* during cold storage (Fig. 5), it could be speculated that the rupture of cellular membrane system removed the structural barrier for SP and Ca<sup>2+</sup> migration and subsequently facilitated the aggregation of SP and PPO zymogens.

### The Melanosis Development of *L. vannamei* During Cold Storage Was Highly Associated with Biochemical Indicators and Cytoarchitecture Degradation

Generally, the heat map gives a good overview of the correlation between multivariable indicators. Thus, the correlations between sensory quality degradation, elevation of PPO and SP activities, alteration of water distribution, and disruption of cytoskeleton in hepatopancreatic tissue of *L. vannamei* during cold storage can be visualized accordingly. As shown in heat map of Fig. 8a, the entire storage periods could be clustered into three stages according to the hierarchical clustering analysis of phenotypic properties. The period from day 0 to day 1 represented the first stage, in which the brightness, sensory score, and T22 amplitude were almost retained at red or orange color, whereas both the PPO and SP activities and shrinkage area displayed blue or green. Consequently, day 2 and day 3 composed the second stage, with moderate alterations in the color scale of brightness, sensory score, PPO and SP activities, free water T23 components, and shrinkage area of cytoarchitecture. Afterwards, day 4 and day 5 formed the third stage, during which the color scale of brightness, sensory score, and T22 amplitude transformed from red or orange to blue or green. On the contrary, the color scale of PPO and SP activities, T23 amplitude, and shrinkage area turned from blue or green to red or orange. Obviously, the overall heat map analysis revealed that the deterioration in brightness and the

**Fig. 7** Migration alteration SP and  $Ca^{2+}$  in *L. vannamei* hepatopancreatic tubule tissue during cold storage for 5 days' storage. **a** Immunohistochemical localization of SP, the black arrows point to the necrocytosis and the dissemination of SP components. **b** Immunofluorescence localization of  $Ca^{2+}$ , the orange arrows point to the necrocytosis and the dissemination of  $Ca^{2+}$

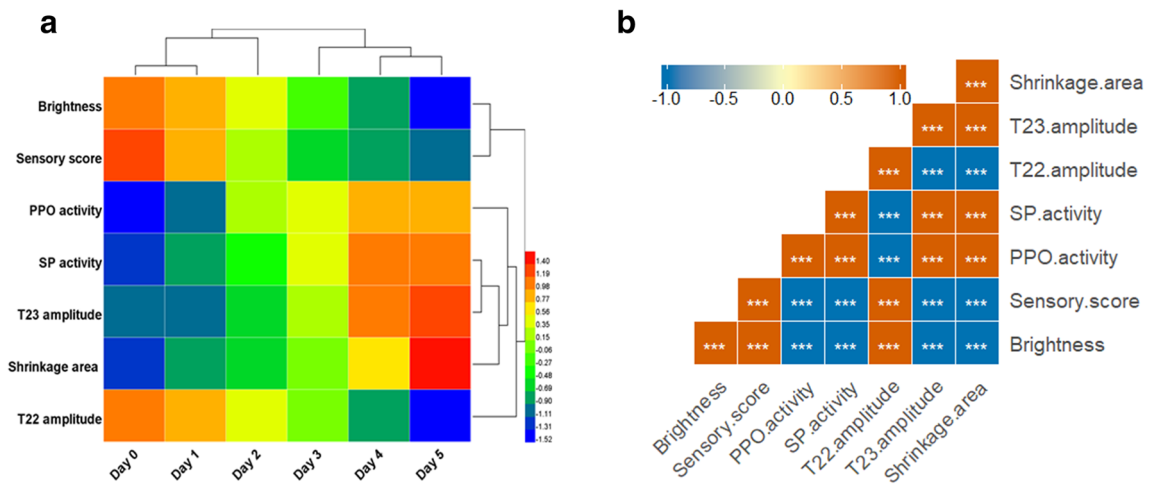
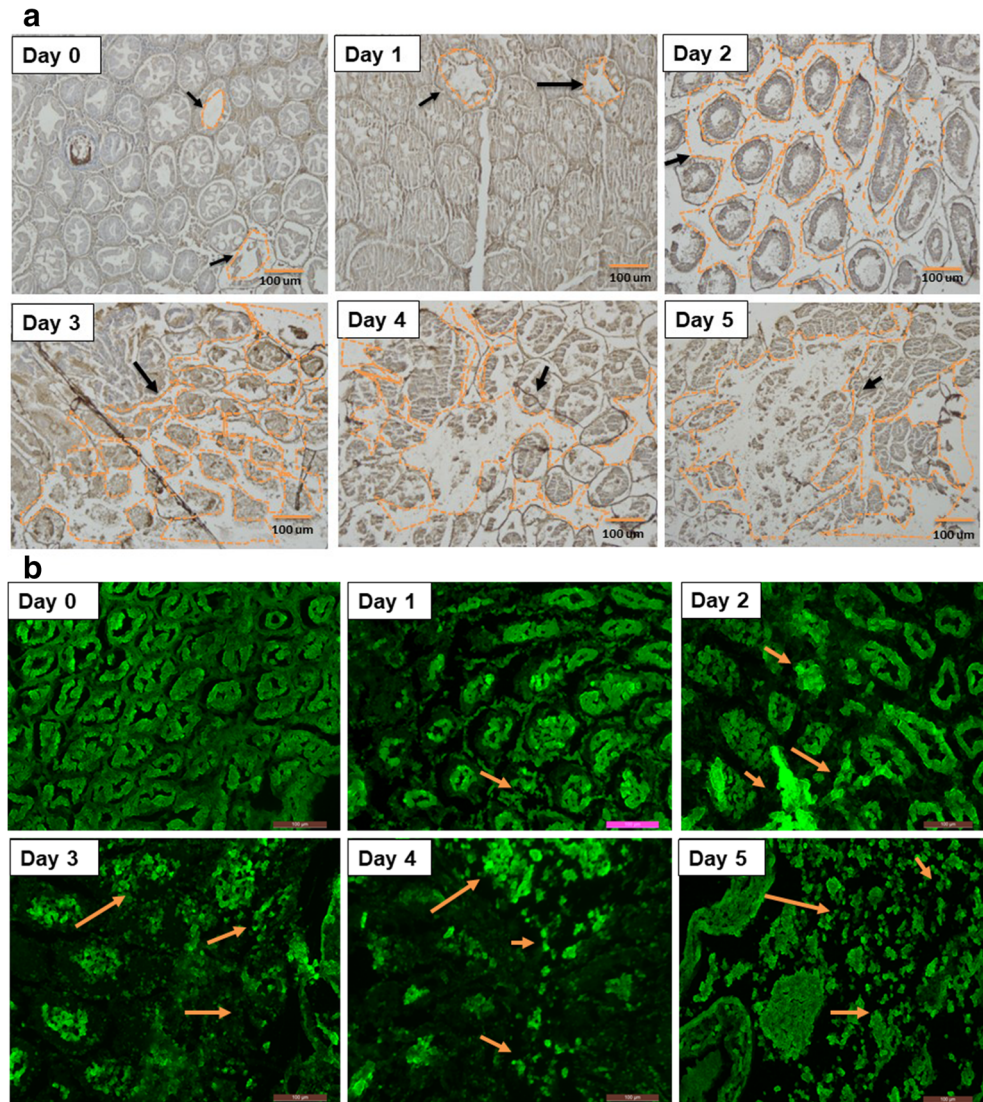


**Fig. 8** Heat map analysis of melanosis development and biochemical indicators. **a** Hierarchical clustering analysis; **b** visualization of correlation analysis. The marks of \*, \*\*, and \*\*\* denote significant

differences as compared with the initial day at  $P < 0.05$ ,  $P < 0.01$ , and  $P < 0.001$  levels, respectively

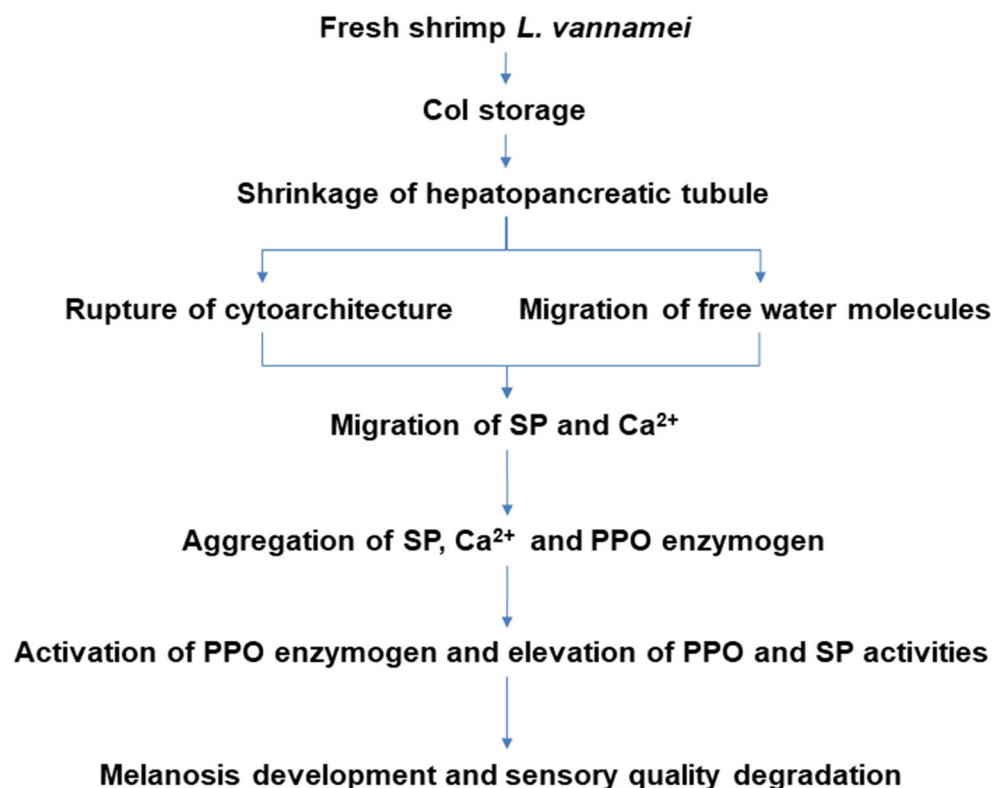
sensory score was positively associated with the elevation of PPO and SP activities, augmentation of free water molecule components, and enlargement of disruption area in intercellular connections. The above results definitely indicated that the melanization of *L. vannamei* during cold storage was largely due to the activation of PPO zymogens and the rupture of tissue cytoarchitectures. These findings are highly consistent with previous reports (Arancibia et al. 2015; Encarnacion et al. 2012; Gokoglu and Yerlikaya 2008).

To further understand the biochemical and cytoarchitectural mechanism inducing melanosis development of *L. vannamei* during cold storage, the correlation analysis between brightness, sensory score, PPO and SP activities, distribution of water components, and cytoarchitectural shrinkage was conducted using the Pearson correlation analysis. As illustrated in Fig. 8b, brightness, the indicator of melanosis development, had a significantly positive correlation with sensory score and T22 amplitude, whereas the negative correlations between brightness and PPO and SP activities, T23 amplitude, and shrinkage area were found ( $P < 0.001$ ). In addition, this result showed high correlations between brightness and the sensory score, indicating brightness the proper indicator to evaluate shrimp freshness. Notably, SP not only plays a vital role in the activation of PPO zymogens but also facilitates the hydrolysis of the cellular framework. Hu et al. (2012) and Singh and Benjakul (2018) demonstrated the participation of endogenous SP in degradation of myofibrillar proteins in fish muscle. In this study, the

Pearson analysis revealed a significant correlation between SP and shrinkage area ( $P < 0.001$ ). Thus, the elevation of SP certainly aggravated the disintegration of cytoarchitectures, following with the enlargement of shrinkage area. Overall, this finding provides a basis for further understanding the cytoarchitecture mechanism of melanosis development in *L. vannamei* during cold storage.

At present, there is little knowledge about the relation of SP activities with the activation level of PPO zymogens after postmortem. In this study, the biochemical and cytoarchitecture mechanisms of *L. vannamei* melanosis development during cold storage were completely elucidated. The results of morphological observation and enzyme activity determination showed that shrimp cephalothorax was more subjective to melanization than abdomen and stern segments, and melanosis development was highly associated with the SP activity in hepatopancreatic tissue. With storage proceeding, the structure integrity of cellular membrane system in hepatopancreatic tissue was gradually destroyed and the barrier structure for restricting migration of free water molecules was accordingly removed off. As a result, owing to the removal of structure barrier and migration of free water molecules, SP and  $\text{Ca}^{2+}$  migrated from hepatopancreatic tissue towards gill and then mediated the activation of PPO zymogen. Altogether, to clearly illustrate the biochemical and cytoarchitectural mechanism of melanosis development in *L. vannamei* during cold storage, the schematic diagram was presented in Fig. 9.

**Fig. 9** Schematic diagram of melanosis development triggered and accelerated by SP-mediated PPO activation in *L. vannamei* during cold storage



## Conclusion

The utmost melanosis development of *L. vannamei* during cold storage is observed at the cephalothorax segments on day 3. The excessive activation of PPO zymogens is closely associated with the increase of SP activity. Furthermore, histochemical and microscopy results reveal that the hepatopancreas tissue undergoes a gradual disruption during cold storage. In combination with the cytoskeleton disruption and migration of free water molecules, the SP and  $\text{Ca}^{2+}$  in hepatopancreas tissue are driven to migrate towards extracellular space, facilitating the aggregation and activation of SP and PPO zymogens. The visualization of correlation analysis further demonstrates that the melanosis development was highly correlated with the biochemical and cytoarchitecture degradation. These findings provide a theoretical basis for further understanding the biochemical and cytoarchitecture mechanism of melanosis development in *L. vannamei* during cold storage and are favorable to conceptualizing innovative strategies against melanization.

**Funding Information** The authors received financial support from the National Natural Science Foundation (No. 31201309, 31772048 and 31371777) and the Key Laboratory of Aquatic Products Processing, Ministry of Agriculture, South China Sea Fisheries Research Institute Key Laboratory of Fishery Products Processing, Ministry of Agriculture, People's Republic of China (No. NYJG201404) and the Natural Science Foundation of Guangdong Ocean University (No. C16396).

## Compliance with Ethical Standards

**Conflict of Interest** The authors declare that they have no competing interests.

## References

- Ahn, C. W., Lee, M. J., & Jeung, E. B. (2017). Expression and localization of equine tissue-specific divalent ion-transporting channel proteins. *Journal of Equine Veterinary Science*, *59*, 14–25.
- Alparslan, Y., & Baygar, T. (2017). Effect of chitosan film coating combined with orange peel essential oil on the shelf life of deepwater pink shrimp. *Food Bioprocess Technology*, *10*, 842–853.
- Amparyup, P., Jitvaropas, R., Pulsook, N., & Tassanakajon, A. (2007). Molecular cloning, characterization and expression of a masquerade-like serine proteinase homologue from black tiger shrimp *Penaeus monodon*. *Fish & Shellfish Immunology*, *22*, 535–546.
- Arancibia, M. Y., Lopez-Caballero, M. E., Gomez-Guill, M. C., & Montero, P. (2015). Chitosan coatings enriched with active shrimp waste for shrimp preservation. *Food Control*, *54*, 259–266.
- Benjakul, S., Visessanguan, W., & Tanaka, M. (2005). Properties of phenoloxidase isolated from the cephalothorax of kuruma prawn (*Penaeus japonicus*). *Journal of Food Biochemistry*, *29*, 470–485.
- Bradford, M. (1976). A rapid and sensitive method for the quantitation of microgram quantities of protein utilizing a principle of protein-dye binding. *Analytical Biochemistry*, *72*, 248–254.
- Buda, S., Elizabeth, S., & Thomas, H. (2005). Expression of a serine proteinase homolog prophenoloxidase-activating factor from the blue crab, *Callinectes sapidus*. *Comparative Biochemistry and Physiology. part: B*, *140*, 521–531.
- Chiu, C. H., Gu, Y. K., Liu, C. H., Pan, T. M., & Cheng, W. (2007). Immune responses and gene expression in Pacific white shrimps, *Litopenaeus vannamei*, induced by *Lactobacillus plantarum*. *Fish & Shellfish Immunology*, *23*, 364–377.
- Dai, X. Y., Zhang, M. X., Wei, X. Y., Hider, R. C., & Zhou, T. (2016). Novel multifunctional hydroxypyridinone derivatives as potential shrimp preservatives. *Food Bioprocess Technology*, *9*, 1079–1088.
- Encarnacion, A. B., Orapint, F. F., Wanchai, J., Ikuo, W., & Toshiaki, H. O. (2012). Application of ergothioneine-rich extract from an edible mushroom *Flammulina velutipes* for melanosis prevention in shrimp, *Penaeus monodon* and *Litopenaeus vannamei*. *Food Research International*, *45*, 232–237.
- Erikson, U., Veliyulin, E., Singstad, T. E., & Aursand, M. (2004). Salting and desalting of fresh and frozen-thawed cod (*Gadus morhua*) fillets: a comparative study using  $^{23}\text{Na}$  NMR,  $^{23}\text{Na}$  MRI, low-field  $^1\text{H}$  NMR, and physicochemical analytical methods. *Journal of Food Science*, *69*, 107–114.
- Geng, S., Wang, H., Wang, X., Ma, X., Xiao, S., Wang, & Tan, J. M. (2015). A non-invasive NMR and MRI method to analyze the rehydration of dried sea cucumber. *Analytical Methods*, *7*, 2413–2419.
- Gokoglu, N., & Yerlikaya, P. (2008). Inhibition effects of grape seed extracts on melanosis formation in shrimp (*Parapenaeus longirostris*). *International Journal of Food Science & Technology*, *43*, 1004–1008.
- Han, M. Y., Wang, P., Xu, X. L., & Zhou, G. H. (2014). Low-field NMR study of heat-induced gelation of pork myofibrillar proteins and its relationship with microstructural characteristics. *Food Research International*, *62*, 1175–1182.
- Hu, Y., Ji, R., Jiang, H., Zhang, J., Chen, J., & Ye, X. (2012). Participation of cathepsin L in modori phenomenon in carp (*Cyprinus carpio*) surimi gel. *Food Chemistry*, *134*, 2014–2020.
- Jiang, H. B., Wang, Y., Yu, X. Q., Zhu, Y. F., & Kanost, M. (2003). Prophenoloxidase-activating proteinase-3 (PAP-3) from *Manduca sexta* hemolymph: a clip-domain serine proteinase regulated by serpin-1J and serine proteinase homologs. *Insect Biochemistry and Molecular Biology*, *33*, 1049–1060.
- José-Pablo, Z., Martínez-Álvarez, O., Montero, P., & del Gómez-Guillén, C. M. (2009). Characterisation and tissue distribution of polyphenol oxidase of deepwater pink shrimp (*Parapenaeus longirostris*). *Food Chemistry*, *112*, 104–111.
- Kaur, B. P., Kaushik, N., Rao, P. S., & Chauhan, O. P. (2013). Effect of high-pressure processing on physical, biochemical, and microbiological characteristics of black tiger shrimp (*Penaeus monodon*). *Food Bioprocess Technology*, *6*, 1390–1400.
- Li, E. C., Chen, L. Q., Zeng, C. N., Yu, Z. Q., Xiong, Chen, X. F., & Qin, J. G. (2008). Comparison of digestive and antioxidant enzymes activities, haemolymph oxyhemocyanin contents and hepatopancreas histology of white shrimp, *Litopenaeus vannamei*, at various salinities. *Aquaculture*, *274*, 80–86.
- Li, C. B., Liu, D. Y., Zhou, G. H., Xu, X. L., Qi, J., Shi, P. L., & Xia, T. L. (2012). Meat quality and cooking attributes of thawed pork with different low field NMR T21. *Meat Science*, *92*, 79–83.
- Li, M., Li, B., & Zhang, W. J. (2018). Rapid and non-invasive detection and imaging of the hydrocolloid-injected prawns with low-field NMR and MRI. *Food Chemistry*, *242*, 16–21.
- Liu, Y. J., Hou, F. J., Wang, X. Z., & Liu, X. L. (2015a). Recombinant expression and characterization of a serine protease inhibitor (Lvserpin 7) from the Pacific white shrimp, *Litopenaeus vannamei*. *Fish & Shellfish Immunology*, *42*, 256–263.
- Liu, P. F., Liu, Q. H., Wu, Y., & Jie, H. (2015b). A pilot metabolic profiling study in hepatopancreas of *Litopenaeus vannamei* with white spot syndrome virus based on  $^1\text{H}$ -NMR spectroscopy. *Journal of Invertebrate Pathology*, *124*, 51–56.

- Liu, Y. J., Liu, T., Hou, F. J., Wang, X. Z., & Liu, X. L. (2016). Lvserpin 3 is involved in shrimp innate immunity via the inhibition of bacterial proteases and proteases involved in prophenoloxidase system. *Fish & Shellfish Immunology*, *48*, 128–135.
- Liu, Y. J., Sun, Y. H., Wang, Q., Hou, F. J., & Liu, X. L. (2017). Identification and functional characterizations of serpin 8, a potential prophenoloxidase-activating protease inhibitor in Pacific white shrimp, *Litopenaeus vannamei*. *Fish & Shellfish Immunology*, *60*, 492–501.
- Lopez-Caballero, M., Martínez-Alvarez, O., Gomez-Guillen, M., & Montero, P. (2007). Quality of thawed deepwater pink shrimp (*Parapenaeus longirostris*) treated with melanosis-inhibiting formulations during chilled storage. *International Journal of Food Science & Technology*, *42*, 1029–1038.
- Luna-Acosta, A., Thomas-Guyon, H., Amari, M., Rosenfeld, E., Bustamante, P., & Fruitier-Arnaudin, I. (2011). Differential tissue distribution and specificity of phenoloxidases from the Pacific oyster *Crassostrea gigas*. *Comparative Biochemistry and Physiology Part: B*, *159*, 220–226.
- Manheem, K., Benjakul, S., Kijroongrojana, K., & Visessanguan, W. (2012). The effect of heating conditions on polyphenol oxidase, proteases and melanosis in pre-cooked Pacific white shrimp during refrigerated storage. *Food Chemistry*, *131*, 1370–1375.
- Montero, P., Lopez-Caballero, M. E., & Perez-Mateos, M. (2001). The effect of inhibitors and high-pressure treatment to prevent melanosis and microbial growth on chilled prawns (*Penaeus japonicus*). *Journal of Food Science*, *66*, 1201–1206.
- Nirmal, N. P., & Benjaku, S. (2009). Effect of ferulic acid on inhibition of polyphenoloxidase and quality changes of Pacific white shrimp (*Litopenaeus vannamei*) during iced storage. *Food Chemistry*, *116*, 323–331.
- Nunes, E. T., Braga, A. A., & Camargo-Mathias, M. I. (2014). Histochemical study of the hepatopancreas in adult females of the pink-shrimp *Farfantepenaeus brasiliensis* Latreille, 1817. *Acta Histochemistry*, *116*, 243–251.
- Perazzolo, M. L., & Barracco, A. M. (1997). The prophenoloxidase activating system of the shrimp *Penaeus paulensi* and associated factors. *Developmental and Comparative Immunology*, *21*, 385–395.
- Reis, C. V., Kelen, E. M. A., Farsky, S. H. P., Portaro, F. C. V., Sampaio, C. A. M., Fernandes, B. L. A. C., Camargo, M., & Chudzinski-Tavassi, A. M. A. (1999). Ca<sup>2+</sup> activated serine protease (LOPAP) could be responsible for the hemorrhagic syndrome caused by the caterpillar *Lononia oblique*. *Lancet*, *353*, 1942.
- Romano, N., Koh, C. B., & Ng, W. K. (2015). Dietary microencapsulated organic acids blend enhances growth, phosphorus utilization, immune response, hepatopancreatic integrity and resistance against *Vibrio harveyi* in white shrimp, *Litopenaeus vannamei*. *Aquaculture*, *435*, 228–236.
- Sánchez-Alonso, I., Martínez, I., Sánchez-Valencia, J., & Careche, M. (2012). Estimation of freezing storage time and quality changes in hake (*Merluccius merluccius*, L.) by low field NMR. *Food Chemistry*, *135*, 1626–1634.
- Sánchez-Alonso, I., Moreno, P., & Careche, M. (2014). Low field nuclear magnetic resonance (LF-NMR) relaxometry in hake (*Merluccius merluccius*, L.) muscle after different freezing and storage conditions. *Food Chemistry*, *153*, 250–257.
- Sánchez-Valencia, J., Sánchez-Alonso, I., Martínez, I., & Careche, M. (2014). Estimation of frozen storage time or temperature by kinetic modeling of the Kramer shear resistance and water holding capacity (WHC) of hake (*Merluccius merluccius*, L.) muscle. *Journal of Food Engineering*, *120*, 37–43.
- Shao, J. H., Deng, Y. M., Song, L., Batur, A., Jia, N., & Liu, D. Y. (2016). Investigation the effects of protein hydration states on the mobility water and fat in meat batters by LF-NMR technique. *LWT-Food Science Technology*, *66*, 1–6.
- Singh, A., & Benjakul, S. (2018). Proteolysis and its control using protease inhibitors in fish and fish products: a review. *Comprehensive Review in Food Science and Food Safety*, *17*, 496–509.
- Somprasong, N., Rimphanitchayakit, V., & Tassanakajon, A. (2006). A five-domain Kazal-type serine proteinase inhibitor from black tiger shrimp *Penaeus monodon* and its inhibitory activities. *Developmental & Comparative Immunology*, *30*, 998–1008.
- Visetnan, S., Donpudsa, S., & Supungul, P. A. (2009). Tassanakajon, V. Rimphanitchayakit, Kazal-type serine proteinase inhibitors from the black tiger shrimp *Penaeus monodon* and the inhibitory activities of SPIPm4 and 5. *Fish & Shellfish Immunology*, *27*, 266–274.
- Wang, Y. B., Liu, L., Zhou, J. R., Ruan, X. M., Lin, J. D., & Fu, L. L. (2015a). Effect of chitosan nanoparticle coatings on the quality changes of postharvest white leg shrimp, *Litopenaeus vannamei*, during storage at 4 °C. *Food Bioprocess Technology*, *8*, 907–915.
- Wang, M., Wang, J. J., Sun, X. H., Pan, Y. J., & Zhao, Y. (2015b). Preliminary mechanism of acidic electrolyzed water ice on improving the quality and safety of shrimp. *Food Chemistry*, *176*, 333–341.
- Wu, J. P., Chen, H. C., & Huang, D. J. (2008). Histopathological and biochemical evidence of hepatopancreatic toxicity caused by cadmium and zinc in the white shrimp, *Litopenaeus vannamei*. *Chemosphere*, *73*, 1019–1026.
- Xu, Z. H., Regenstein, J. M., Xie, D. D., Lu, W. J., Ren, X. C., Yuan, J. J., & Mao, L. C. (2018a). The oxidative stress and antioxidant responses of *Litopenaeus vannamei* to low temperature and air exposure. *Fish & Shellfish Immunology*, *72*, 564–571.
- Xu, D. F., Sun, L. J., Li, C. H., Wang, Y. L., & Ye, R. Y. (2018b). Inhibitory effect of glucose oxidase from *Bacillus sp.* CAMT22370 on the quality deterioration of Pacific white shrimp during cold storage. *LWT-Food Science and Technology*, *92*, 339–346.

**Publisher's Note** Springer Nature remains neutral with regard to jurisdictional claims in published maps and institutional affiliations.